

# Computer-Aided Design and Simulation of TiO<sub>2</sub> Micro-Ring Resonator

Payal Verma<sup>\* \*\*</sup>, S.A. Degtyarev<sup>\*\*</sup>, A.N.K. Reddy<sup>\*\*</sup>, S.A. Fomchenkov<sup>\*\*</sup>, V.S. Pavelyev<sup>\*\*</sup> and S.N. Khonina<sup>\*\*</sup>

<sup>\*</sup>Department of Electronics and Communication Engineering, M.V. J. College of Engineering, Bangalore - 560067, India  
Email: payalsedha@gmail.com; payal.verma@mvjce.edu.in

<sup>\*\*</sup>Samara National Research University (Samara University), 34, Moskovskoye Shosse, Samara - 443086, Russia  
Email: sealek@gmail.com; naareddy@gmail.com; s.a.fom@mail.ru; pavelyev10@mail.ru; khonina@smr.ru

**Abstract:** In this paper, we present the results of three dimensional full-vector static electromagnetic simulation of silicon micro-ring resonator operation. It is shown in the paper that geometrical and scalar approaches are not sufficiently accurate for calculating resonator parameters. Quite strong dependence of ring resonator radius on waveguide width is revealed.

**Keywords:** Micro-ring resonator, COMSOL, Electro optical, Optical filtering, Full-3D numerical simulation.

## Introduction

This document is a template. An electronic copy can be downloaded from the conference website. For questions on paper guidelines, please contact the conference publications committee as indicated on the conference website. Information about final paper submission is available from the conference website. Resonant optical structures are promising and find widespread application in the field of optical data and signal processing. The principles of optical data processing for analog optical computers are described in paper [1]. There are adding optical elements, differentiators and integrators, amplifiers, optical filtering elements, and others. Several structures have been used for optical logical elements. Some of such resonant structures are Microfiber elements [2], diffractive optical elements (DOEs) [3, 4], Bragg structures [5, 6], photonic crystals [7], and their different combinations [8]. Optical signal integration using Optical-fiber photonic crystal resonator is presented in paper [9], where the resonant parameters have been calculated.

Apart from the above mentioned optical logical elements for signal processing, 3-D optical-waveguide devices based on micro-ring resonators [10] can be considered as the most appropriate elements for optical integrated circuits. Micro-ring resonators can be the principal elements in filtering arrangements [2], modulators [11], OR-, AND-, XNOR-type logical elements [12], electro-optical and acoustic-optical modulators and switches [13], thermo sensitive resonators [14].

The application of micro-ring resonators are not limited to those mentioned above. Ring resonator structure is also used in highly sensitive sensors of biological liquids [15, 16], acoustic sensors [17], poison gases sensors [18, 19], accelerometers [20], temperature sensors, and various other sensors.

Micro-ring resonators are operationally flexible, relatively compact, and quite noise resistant, these being the reasons for its applicability in several fields. An added advantage is that they can be manufactured with traditional microelectronics and diffractive optics technologies. However, there are certain challenges in the design of the resonator since it involves lot of parameters that should be taken into account during 3-D simulation of the device. In order to closely simulate the device, parameters such as wavelength, full electric amplitude vector, big sizes, and so on should be taken into account deliberately. In this paper we present the simulation of the micro-ring resonator carefully considering the various parameters with an aim of optimization of the parameters. The device has been simulated using COMSOL Multi-physics software. A scheme of simulated micro-ring resonator is shown in Fig.1.

## Concept and Parameters

The concept of the micro ring resonator design is presented here. The diameter of resonator should correspond to the resonant frequency of ring waveguide. In that case the waveguide ring absorbs a wave with resonant wavelength. According to paper [21], the resonant condition is  $kn(L_1 + L_2) = \pi m$ ,  $m = 1, 2, \dots$ , here  $L_1$  – coupling part of the ring,  $L_2$  – propagating part of the ring without coupling. Coupling coefficient and resonator quality-factor depends on the distance between the coupling part and input and output waveguides. In addition, total internal condition should be satisfied for the ring. In order to meet this criterion, the material of the ring should have a high refractive index. The most commonly used material with high refractive index is silicon or a more promising candidate would be titanium dioxide.

The simulated ring resonator device has the following parameters: gap  $g = 100$  nm, wavelength  $\lambda = 1556.9$  nm, height of structure  $h = 220$  nm, width of the waveguide  $a = 540$  nm. For the sake of simplification, the structure is assumed to be in

vacuum. For the chosen wavelength, refractive index of  $\text{TiO}_2$ ,  $n = 2.4324$ . As explained above, radius of the ring should be chosen such that the optical path in ring should include integer number of wavelengths. That is  $R = m\lambda/2\pi n$ , here  $m$  is number of wavelengths which are packed in the ring. Thus,  $R = 2037.4$  nm if  $m = 20$ ,  $R = 2139.2677$  nm if  $m = 21$  and  $R = 2241.13$  nm if  $m = 22$ . This formula for the radius of resonator is approximate because the ring has a non-zero width. In the present work the radius is considered as the distance from the centre to the middle of ring waveguide as shown in Fig. 1a. Notice that the mode of the ring waveguide can be slightly decentred relative to the centre of the waveguide. Thus, resonance radius can differ from the meaning which is calculated with the mentioned formula.

This has been observed during resonance simulation using COMSOL software. In the present work we create a scheme from Fig. 1b. and we reveal that if the radius of ring resonator is calculated with approximate formula, there is no resonance. In order to find the resonance radius we vary the theoretically calculated meaning.

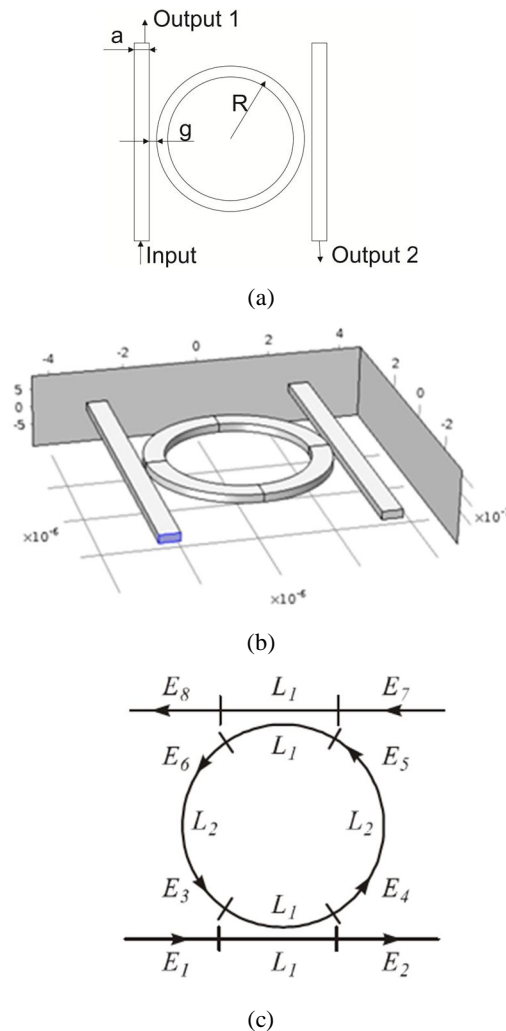
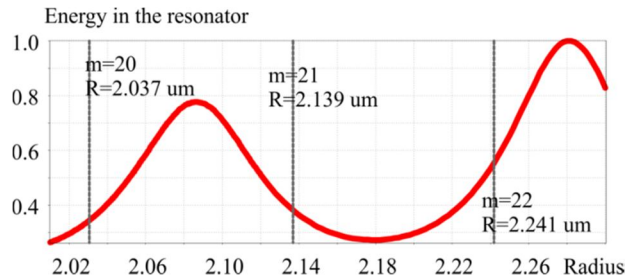


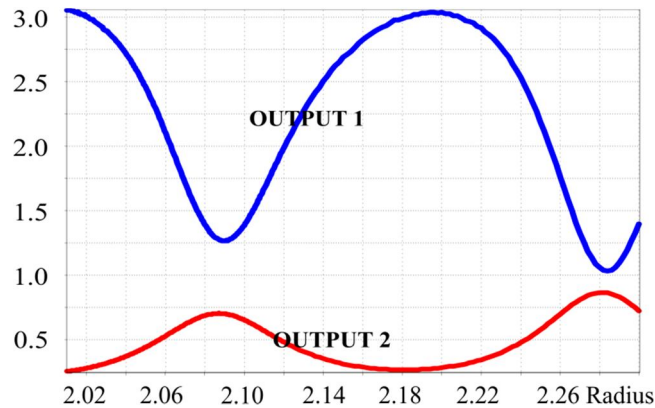
Figure 1. (a) Scheme of a ring resonator; (b) 3d scheme and (c) scheme of resonance ring waveguides coupling

## Result and Discussion

In Fig. 2a, accumulated energy is shown against the resonance radius, where the red line represents energy which accumulates in the resonator. The geometrically calculated resonance radii are represented by the vertical grey dashed lines and the Red line is plotted based on COMSOL simulation. We can see that the maximum values of the red lines are not equal over the geometrically calculated radii. The first resonant radius is  $R = 2088.5$  nm and the second resonant radius is  $R = 2280$  nm, whereas geometrically calculated radii are  $R = 2037.4$  nm when  $m = 20$ ,  $R = 2139.2677$  nm when  $m = 21$  and  $R = 2241.13$  nm when  $m = 22$ . In Figure 2b, the output intensity is plotted versus the resonator radius. It can be observed from the plot that the intensity at output 2 is maximal for resonant radii.



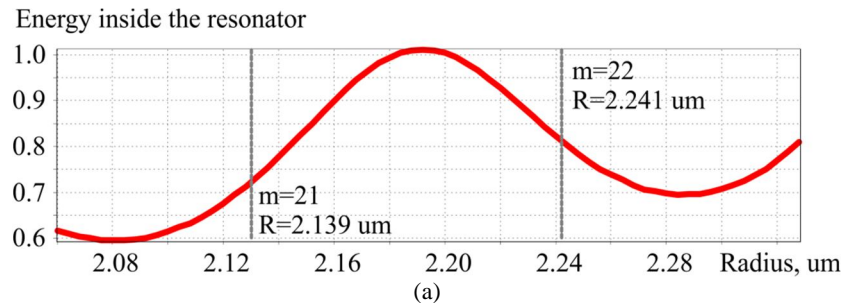
(a)



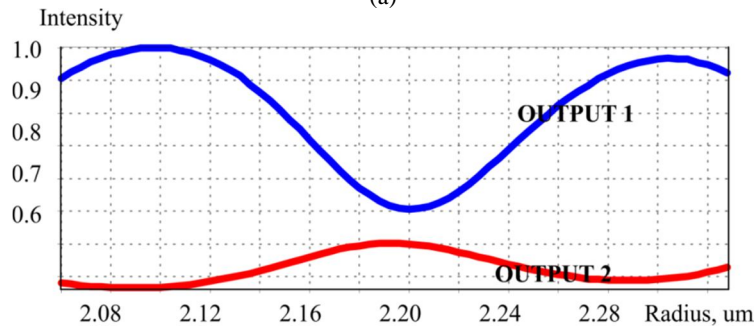
(b)

Figure 2. Energy characteristics of resonator for different radii of the ring: (a) Energy inside the ring: intensities in the outputs (2); (b) Energy inside the ring: intensities in the outputs (1) & (2); width of the resonator is 540 nm

Energy characteristics of the ring resonator with 500 nm radius are shown in Fig. 3.



(a)



(b)

Figure 3. Energy characteristics of resonator for different radii of the ring: (a) Energy inside the ring: intensities in the outputs (2); (b) Energy inside the ring: intensities in the outputs (1) & (2); width of the resonator is 500 nm

Energy characteristics of the ring resonator with 460 nm radius are shown in Fig. 4.

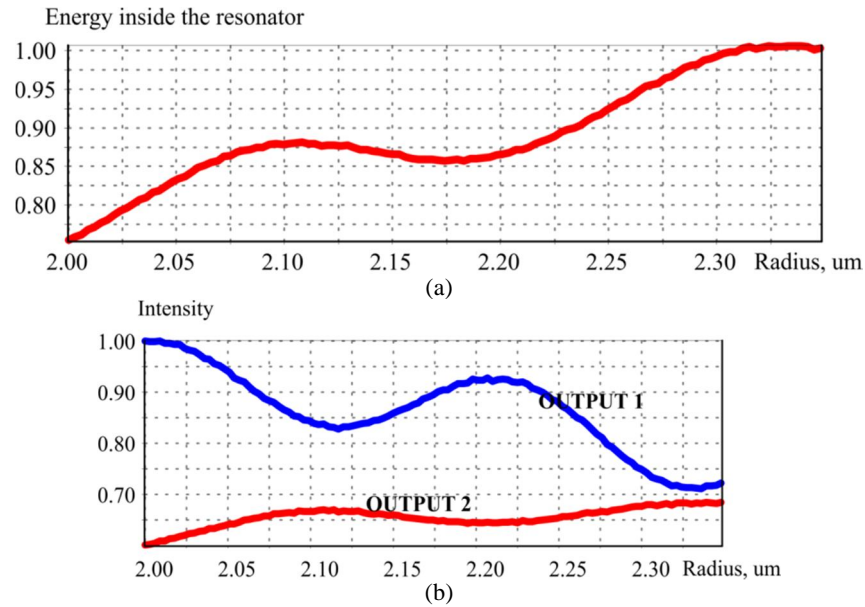


Figure 4. Energy characteristics of resonator for different radii of the ring: (a) Energy inside the ring: intensities in the outputs (2); (b) Energy inside the ring: intensities in the outputs (1) & (2); width of the resonator is 460 nm

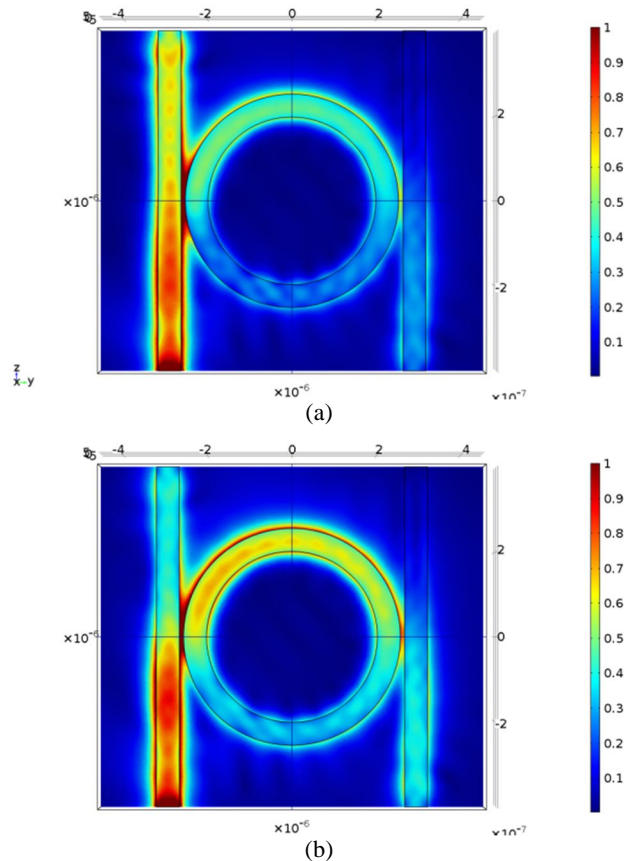


Figure 5. Electric amplitude distribution in microring resonator: (a) R = 2241 nm; (b) R = 2280 nm; waveguide width is 540 nm

The Electric amplitude distribution in microring resonator for different radii is shown in Fig. 5. It can be seen that the intensity at output 2 in Fig. 5b is significantly greater than the intensity at the output 2 in Fig. 5a. Thus, the simulated data using COMSOL software provides more accurate resonant meanings of ring resonator radius compared to the theoretically calculated meaning.

Table 1. Evaluation of the influence of waveguide width  $a$  to resonant radius of the waveguide

Waveguide width $a$ (Fig. 1a)	Resonant radii $R$ (Fig. 1a)
540 nm	2088.5 nm, 2280 nm
500 nm	2192 nm
460 nm	2108 nm, 2336 nm

## Conclusions

This paper is devoted to 3d full-vector static electromagnetic simulation of TiO<sub>2</sub> micro-ring resonator operation. The design parameters used for the device have been presented. The theoretically calculated resonant meaning of the ring resonator has been compared with simulated results. The energy characteristics and Electric amplitude distribution data for different radii has been studied and presented. With the results of this paper, we reveal that geometrical and scalar approaches are not sufficiently accurate for calculating resonator parameters. Simulations carried out using COMSOL software reveal that geometrically calculated radii are not resonant. In addition, meanings of resonant radii are dependent on the width,  $a$ , of the waveguide. Geometrical approach does not take into consideration the width,  $a$ , at all. Hence, there is discrepancy between the theoretical and simulated results. It is also shown that, for the total pumping of energy from the first output to the second we need one-mode waveguides as an entrance and output silicon trap and a ring resonator too. Thus, waveguide width,  $a$ , can vary from  $\lambda/2n$  to  $\lambda/n$ . In the present case waveguide width,  $a$ , can vary from 223.7 nm to 447.4 nm. Manufacturing tolerance can be simulated by introducing simple deviations of geometry, sinusoidal relief function, minor ellipticity and so on. At this stage of research work presented in the paper, we could draw few important conclusions mentioned above, that would be helpful for further fabrication and development of TiO<sub>2</sub> ring resonator on substrate.

## Acknowledgment

This work is supported by M.V.J. College of Engineering, Bangalore, India and the Ministry of Education and Science of the Russian Federation.

## References

- [1] Gavrilov, A. V., Soifer, V. A., "Prospects of optical analog computer development," *Computer Optics*, 36(2), 140-150(2012).
- [2] Little, B. E., Chu, S. T., Haus, H. A., Foresi, J. and Laine, J. P., "Microring resonator channel dropping filters," *Journal of lightwave technology*, 15(6), 998-1005(1997).
- [3] Golovastikov, N. V., Bykov, D. A., Doskolovich, L. L., "Resonant diffraction gratings for spatial differentiation of optical beams," *Quantum Electronics*, 44(10), 984(2014).
- [4] Bykov, D. A., Doskolovich, L. L., Golovastikov, N. V. and Soifer, V. A., "Time-domain differentiation of optical pulses in reflection and in transmission using the same resonant grating," *Journal of Optics*, 15(10), 105703 (2013).
- [5] Golovastikov, N. V., Bykov, D. A., Doskolovich, L. L. and Bezus, E. A., "Spatial optical integrator based on phase-shifted Bragg gratings," *Optics Communications*, 338, 457-460 (2015).
- [6] Bykov, D. A., Doskolovich, L. L., Bezus, E. A., Soifer, V. A., "Optical computation of the Laplace operator using phase-shifted Bragg grating," *Optics express*, 22(21), 25084-25092(2014).
- [7] Kazanskiy, N. L., Serafimovich, P. G., Khonina, S. N., "Use of photonic crystal cavities for temporal differentiation of optical signals," *Optics Letters*, 38(7), 1149-1151 (2013).
- [8] De Leonardis, F., Campanella, C. E., Troia, B., Perri, A. G., Passaro, V., "Performance of SOI Bragg grating ring resonator for nonlinear sensing applications," *Sensors*, 14(9), 16017-16034 (2014).
- [9] Kazanskiy, N. L. and Serafimovich, P. G., "Coupled-resonator optical waveguides for temporal integration of optical signals," *Optics Express*, 22(11), 14004-14013 (2014).
- [10] Nishihara, H., Haruna, M., Sahara, T., "Electro-optics handbook" 2nd ed. Chapter 26, Optical integrated circuits, New York (1989).
- [11] Rabiei, P., Steier, W. H., Zhang, C., Dalton, L. R., "Polymer micro-ring filters and modulators," *Journal of lightwave technology*, 20(11), 1968 (2002).
- [12] Van, V., Ibrahim, T. A., Absil, P. P., Johnson, F. G., Grover, R., Ho, P. T., "Optical signal processing using nonlinear semiconductor microring resonators," *IEEE Journal of Selected Topics in Quantum Electronics*, 8(3), 705-713 (2002).
- [13] Guarino, A., Poberaj, G., Rezzonico, D., Degl'Innocenti, R., Günter, P., "Electro-optically tunable microring resonators in lithium niobate," *Nature Photonics*, 1(7), 407-410 (2007).
- [14] Liu, F., Li, Q., Zhang, Z., Qiu, M. and Su, Y., "Optically tunable delay line in silicon microring resonator based on thermal nonlinear effect," *IEEE Journal of Selected Topics in Quantum Electronics*, 14(3), 706-712 (2008).
- [15] Yalcin, A., Popat, K. C., Aldridge, J. C., Desai, T. A., Hryniewicz, J., Chbouki, N., Gill, D., "Optical sensing of biomolecules using microring resonators," *IEEE Journal of Selected Topics in Quantum Electronics*, 12(1), 148-155 (2006).
- [16] De Vos, K., Bartolozzi, I., Schacht, E., Bienstman, P., Baets, R., "Silicon-on-Insulator microring resonator for sensitive and label-free biosensing," *Optics express*, 15(12), 7610-7615 (2007).
- [17] Chao, C. Y., Ashkenazi, S., Huang, S. W., O'Donnell, M., Guo, L. J., "High-frequency ultrasound sensors using polymer microring resonators," *IEEE transactions on ultrasonics, ferroelectrics, and frequency control*, 54(5), 957-965 (2007).

- [18] Passaro, V., Dell'Olio, F., De Leonardi, F., "Ammonia optical sensing by microring resonators," *Sensors*, 7(11), 2741-2749 (2007).
- [19] Robinson, J. T., Chen, L., & Lipson, M., "On-chip gas detection in silicon optical microcavities," *Optics Express*, 16(6), 4296-4301(2008).
- [20] Laine, J. P., Tapalian, C., Little, B., Haus, H., "Acceleration sensor based on high-Q optical microsphere resonator and pedestal antiresonant reflecting waveguide coupler," *Sensors and ActuatorsA: Physical*, 93(1), 1-7 (2001).
- [21] Kotlyar V.V., Kovalev A.A., Shuyupova Ya.O., Nalimov A. G., Soifer V.A., "Subwavelength location of light in waveguide structures," *Computer Optics* 34(2), 169-186 (2010).